

INTRODUCTION

Seizures (SZs) and infra-clinical paroxysmal discharges (IPDs) in Focal cortical dysplasia type 2 (FCD2) occur predominantly during sleep. IPDs can resemble the beginning of SZs, but they do not progress into full-fledged clinical seizures. Characterizing and differentiating sleep-related IPDs from SZs may help elucidate the pathophysiological pathways that underlie sleep-related seizures and find more effective treatment strategies.

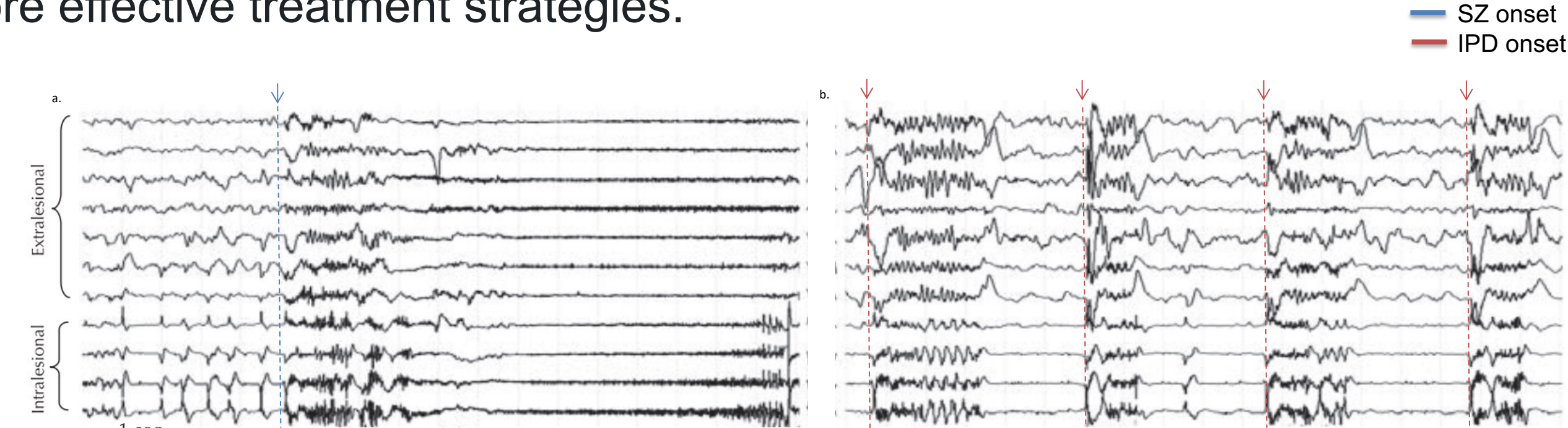


Figure 1: SEEG recordings during sleep. In the lower part, the intracerebral contacts are within the type IIb FCD (intralesional) and, in the upper part, outside (extralesional). a) The onset of a seizure during stage II non-REM sleep. b) During non-REM sleep, FCD activity was pseudo-periodic (about four seconds) and the interictal activity spread to the non-lesional areas. Panels from [1].

Objective

In this study, we aimed to evaluate the level of neuronal dynamics within and outside the Epileptogenic Zone (EZ; the brain area involved in the origin and propagation of seizures), before both IPDs and SZs.

METHODS

Dataset: We acquired overnight stereo-electroencephalography (sEEG) recordings (7 hours) from 14 subjects affected by FCD2 and undergoing pre-surgical clinical assessment. The EZ was visually identified by clinical experts. The region of the brain not involved in seizure origin and propagation was defined as non-EZ. We analyzed 20-minute segments of uninterrupted spontaneous activity pre-SZs (n=18) and pre-IPDs (n=22).

Patterns analysis: We tested different neuronal dynamics within and between EZ and non-EZ sub-networks in 4-minute time windows with 50% overlap. Assessing:

- Neuronal synchronization using the Phase Locking Value (PLV) [2].
- Balance between cortical excitatory and inhibitory activity using the functional excitatory and inhibitory index (fE/I) [3].
- Bistability of neuronal oscillations using the bistability index (BiS).

SYNCHRONIZATION PATTERNS

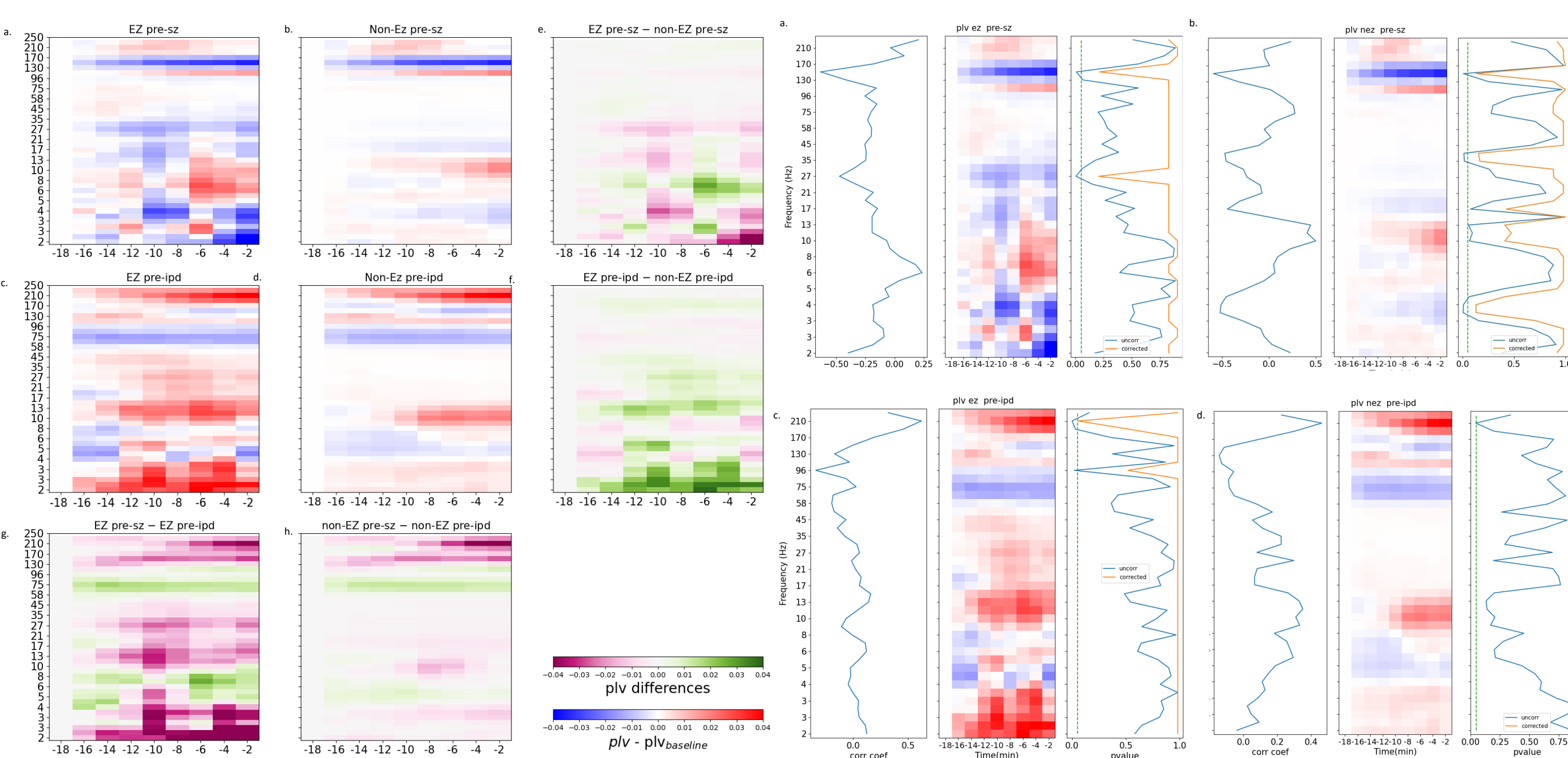


Figure 2: Left panel: Time-frequency PLV normalized with the baseline epoch at 20 min before the event for each condition: a) EZ pre-SZ, b) non-EZ pre-SZ, c) EZ pre-IPD, d) non-EZ pre-IPD. The differences between the matrices first mentioned were calculated and shown respectively in e) EZ – non-EZ pre-SZ, f) EZ – non-EZ pre-IPD, g) EZ pre-SZ – pre-IPD, h) non-EZ pre-SZ – pre-IPD. The other images show the significance of the differences obtained between groups. Right Panel: Correlation coefficient (left), time-frequency PLV normalized with the epoch at 20 min before the event (middle), and p-values (right) - uncorrected in blue, corrected in orange in a) EZ pre-SZ b) non-EZ pre-SZ, c) EZ pre-IPD, d) non-EZ pre-IPD

Pre-SZ:

- Decrease of neuronal synchronization in the localized gamma range characterized by time-related variations in synchrony.
- Increase in neuronal synchronization in the delta-to-alpha frequency range displaying an all-or-nothing response. Even in non-EZ, highlighting the existence and importance of external events outside the EZ.

Pre-IPD:

- Gamma frequencies consistently exhibit reduced synchronization.
- Higher synchronization with significant positive temporal correlation is observed in higher gamma frequencies (210-250Hz) in EZ and non-EZ.

EXCITATION-INHIBITION PATTERNS

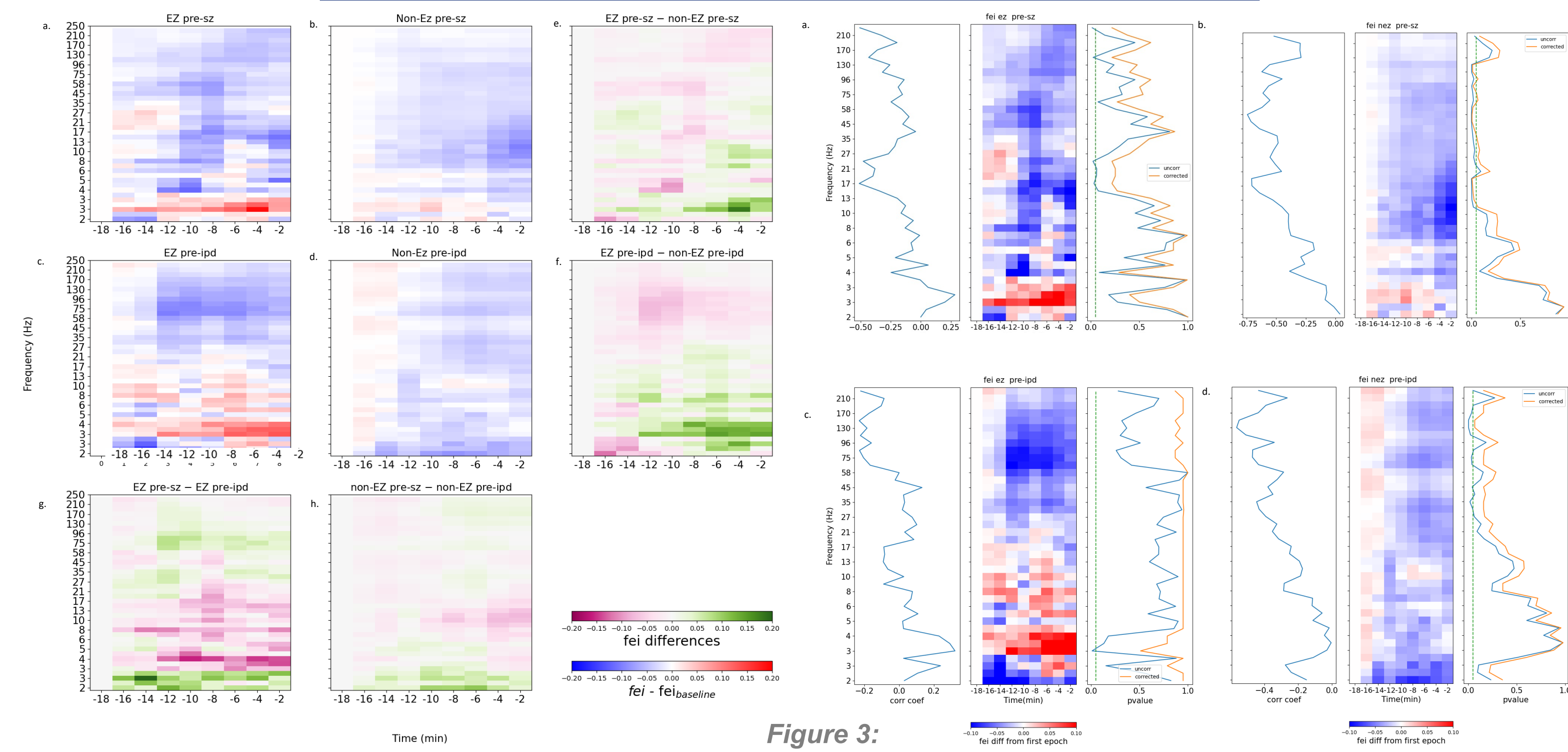


Figure 3: Left panel: Time-frequency PLV (left panel) normalized with the baseline epoch at 20 min before the event for each condition: a) EZ pre-SZ, b) non-EZ pre-SZ, c) EZ pre-IPD, d) non-EZ pre-IPD. The differences between the matrices first mentioned were calculated and shown respectively in e) EZ – non-EZ pre-SZ, f) EZ – non-EZ pre-IPD, g) EZ pre-SZ – pre-IPD, h) non-EZ pre-SZ – pre-IPD. The other images show the significance of the differences obtained between groups. Right Panel: Correlation coefficient (left), time-frequency fE/I normalized with the epoch at 20 min before the event (middle), and p-values (right) - uncorrected in blue, corrected in orange in a) EZ pre-SZ b) non-EZ pre-SZ, c) EZ pre-IPD, d) non-EZ pre-IPD

Pre-SZ:

- Temporally correlated increase in cortical excitability in the delta frequencies, potentially signaling a shift towards epileptic activity within the slow brain oscillations.

Pre-IPD:

- Excitability increases in the theta range, but there is an absence of temporal dynamics.

BISTABILITY PATTERNS

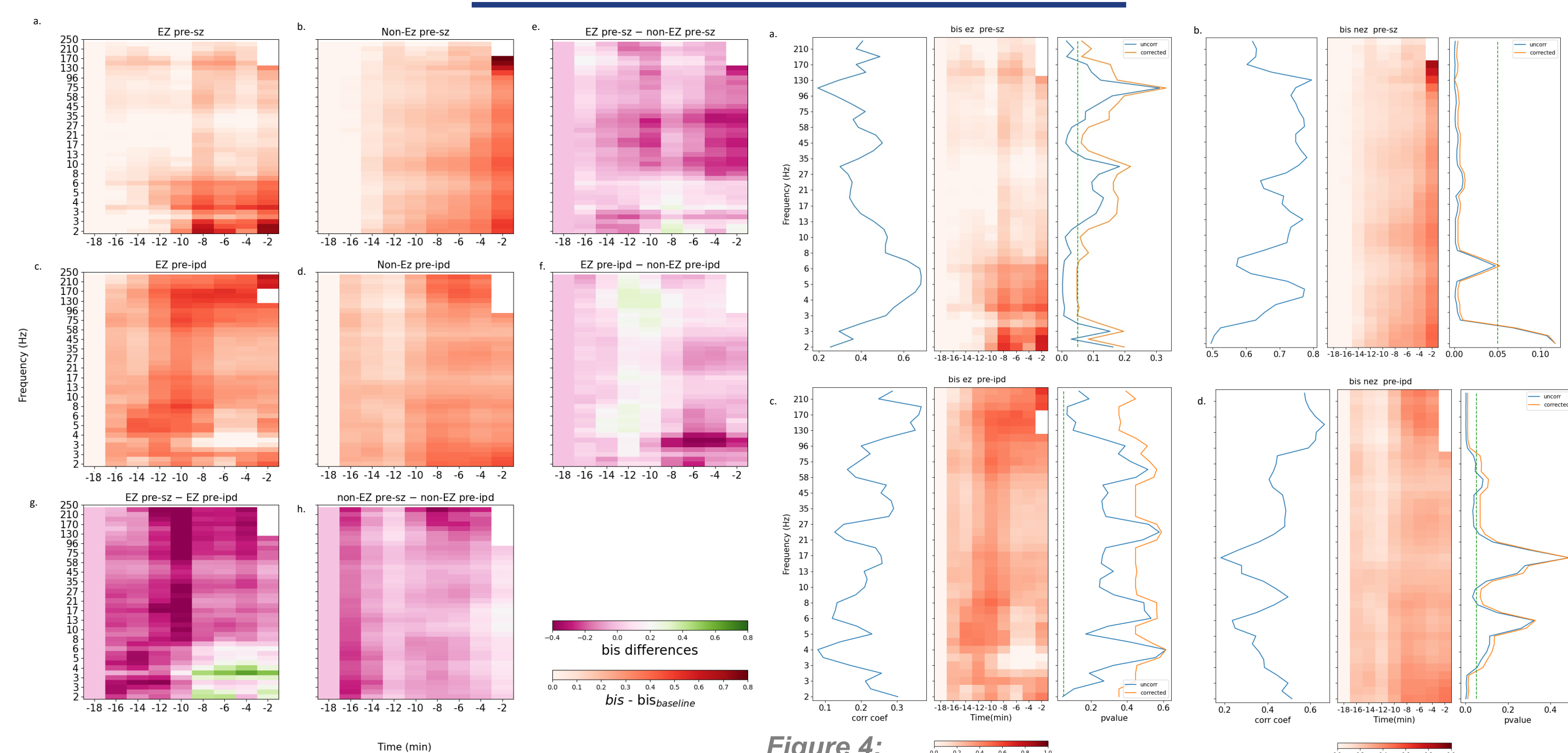


Figure 4: Left panel: Time-frequency PLV (left panel) normalized with the baseline epoch at 20 min before the event for each condition: a) EZ pre-SZ, b) non-EZ pre-SZ, c) EZ pre-IPD, d) non-EZ pre-IPD. The differences between the matrices first mentioned were calculated and shown respectively in e) EZ – non-EZ pre-SZ, f) EZ – non-EZ pre-IPD, g) EZ pre-SZ – pre-IPD, h) non-EZ pre-SZ – pre-IPD. The other images show the significance of the differences obtained between groups. Right panel: Correlation coefficient (left), time-frequency BiS normalized with the epoch at 20 min before the event (middle), and p-values (right) - uncorrected in blue, corrected in orange in a) EZ pre-SZ b) non-EZ pre-SZ, c) EZ pre-IPD, d) non-EZ pre-IPD

Pre-SZ:

- Temporally correlated high increase in bistability, most pronounced in EZ only in the delta to alpha range.

Pre-IPD:

- A less pronounced increase in bistability in all the frequencies.

CONCLUSION

- Temporal correlated patterns in the described metrics go along with temporal uncorrelated behaviors.
- Significance of non-EZ in aiding the propagation of seizures.
- At the onset of a seizure, there are frequency regions where synchronization is lost, and local excitability decreases.
- Bistability always increases approaching both events, especially in the delta to alpha range pre-SZ.

REFERENCES and ACKNOWLEDGMENTS

- [1] L. Tassi, R. Garbelli, N. Colombo, et al., "Electroclinical, MRI and surgical outcomes in 100 epileptic patients with type II FCD," *Epileptic Disorders*, vol. 14 (3), pp. 257–266, Sep. 2012.
- [2] G. Arnulfo, S. H. Wang, V. Myrov, et al., "Long-range phase synchronization of high-frequency oscillations in human cortex," *Nature Communications* 2020 11:1, vol. 11 (1), pp. 1–15, Oct. 2020.
- [3] H. Bruining, R. Hardstone, E. L. Juarez-Martinez, J. Sprengers, A.-E. Avramiea, S. Simpraga, S. J. Houtman, S.-S. Poil, E. Dallares, S. Palva, et al., "Measurement of excitation-inhibition ratio in autism spectrum disorder using critical brain dynamics," *Scientific reports*, vol. 10, no. 1, pp. 1–15, 2020

This work was carried out within the framework of the project: «MNESYS – A multiscale integrated approach to the study of the nervous system in health and disease»